Mercury does not affect F-actin levels in glial cells

Michael Ophir
Independent Research Project
Biology 324- Neurobiology
April 21, 2008

Introduction

The prevalence of mercury in our environment and the extent of its damage on the health of a variety of organisms has been a contentious issue in our society for many decades. There have been many conflicting reports as to how much and in what forms mercury can affect human health. For example, the effect that the presence of mercury in amalgam tooth fillings has on one's health has been a particularly bitterly contested issue. Individuals who are opposed to the incorporation of mercury in dental fillings have argued that the mercury in the filling can vaporize and be inhaled by the lungs, causing the formation and prevalence of mercuric ions in the body and circulatory system (Kindt, et al., 2006). Of course, it has been found that mercury vapor can inhibit the binding of GTP molecules to tubulin, a protein that constitutes microtubules, structures which make up the cellular cytoskeleton (Leong, et al., 2000). The inhibition of GTP binding leads to the inhibition of microtubule polymerization. In turn, it can be inferred that a depletion of microtubule filaments in a cell can significantly affect how the cell behaves and carries out its specific functions within an organism (Leong, et al., 2000). Microtubules play important roles in maintaining cell shape, cell movement, transport of organelles and even separation of chromosomes during cell division (Cooper et al., 2004). If microtubule filaments cannot assemble properly, significant disruptions in physiological processes may occur, thereby completely altering and hindering an organism's development and normal function.

Another important component of the cell cytoskeleton is actin. Actin consists of G-actin (globular actin) subunits, which polymerize to form filamentous actin, also known as F-actin (Cooper, et al., 2004). Actin too plays important roles in maintaining cell shape and structure, supporting the plasma membrane, as well mediating between cell-cell adhesion interactions; many cell adhesion molecules (CAMs) have been found to be linked to the actin cytoskeleton (Cooper, et al., 2004). To better understand the role that actin plays in maintaining cell structure, the mechanism by which it assembles must first be understood.

G-actin subunits have two binding sites specific for other G-actin molecules (Cooper et al., 2004). These monomers can associate with one another and can bind to both the "minus" and "plus" ends of a growing actin filament, but the "plus" end of the actin filament has been shown to elongate much quicker than the "minus" end (Cooper et al., 2004). The mere association and organization into a long straight chain of many G-actin subunits cannot

constitute an actin filament. The associations that occur between the globular actin are too weak amongst themselves for them to withstand the varying sources of strain, pressure and fluctuations in thermal energy that are required in order to prevent filaments from falling apart (Alberts et al., 2002). Rather, it can be said that multiple long actin filaments, known as protofilaments, associate with one another in an end to end fashion such that they are stacked one on top of another laterally, similar to how a brick wall is organized. Initially, a few actin subunits bind with one another in a process known as nucleation, forming a small cluster which is stabilized as a result of many sites of contact of the subunits with one another. This small cluster, or nucleus, serves as the site onto which more actin subunits can bind to or dissociate from, thereby forming a protofilament (Alberts et al., 2002). The protofilaments tend to wrap around each other, generating a sort of helical shape that ensures stability and resistance against breakage that could be induced as a result of fluctuations in temperature, pH and other intracellular environmental factors that surround the actin assemblage (Alberts et al., 2002).

Actin monomers bind to both ends of the growing actin protofilament, although at different rates. Levels of ATP depend on the rate of subunit addition and hydrolysis. If the rate of subunit addition is high, less ATP is hydrolyzed, and thus there is less ADP. These ATP molecules can readily bind to actin subunits. It has been determined that when ATP-associated actin binds to an end of a growing actin filament, normally the “plus” end, its ability to dissociate is much lower than the ability of an ADP-associated actin subunit to dissociate (from the “minus” end). In essence, the rate at which ATP-associated actin is binding to the filament is faster than the rate at which nucleotide hydrolysis, or dissocation, is occuring. In contrast, at the “minus” end, subunit dissociation is faster than subunit binding. Thus, there is a net loss in monomers at the “minus end and a net gain at the “plus” end. This set of events is commonly referred to as treadmilling and highlights the fact that the “plus” end of F-actin seems to polymerize at the same time as the “minus” end loses monomers. This treadmilling effect has been thought to play a crucial role in regulating and adjusting cell shape so as allow for cell mobility and proper cell function. It is believed that mercury disrupts this process by interfering with the association between the ATP and actin monomer at the “plus” end, such that de-polymerization is quicker than the filament can be assembled (Elliget, et al., 1991).

One of the reasons actin plays a major role in conferring cell shape and structural stability is due to the fact that actin nucleation generally occurs at the plasma membrane. As actin polymerizes or de-polymerizes, the cell can undergo changes in its shape that allow it to carry out functions for which it is specific; phagocytosis is one example of such a function (Cooper et al., 2004). Actin nucleation does not occur randomly. Rather, this process is dependent on the interaction between a variety of signals present in a cell’s extracellular environment, and the actin that lies under the plasma membrane of the cell (Alberts et al., 2002). Depending on the signal, actin filaments may be triggered to (de)-

polymerize with the aid of certain proteins. For instance, the Arp2/3 complex of proteins functions by binding close to the "plus" end of an actin filament, and serves as a binding site onto which more ATP-associated actin monomers can bind, thereby forming a new branch of F-actin (Cooper et al., 2004). Furthermore, a protein known as profilin functions to elongate actin filaments by stimulating a trade off of ADP for ATP. Once this trade-off occurs, binding of actin to ATP forms ATP-associated actin that can now bind onto the growing end of actin filaments (Cooper et al., 2004). In contrast, an ADF/cofilin complex functions by increasing the rate at which ADP-associated actin subunits are dissociated from the "minus" end of an actin filament (Cooper et al., 2004). Studies have shown that upon exposure to methylmercury, profilin cannot bind to F-actin and hence, elongation of the filament cannot occur (Elliget, et al., 1991).

Like in the case of microtubules, the exposure of actin to mercury may induce alterations and rearrangements in the actin filaments. For instance, it has been demonstrated that exposure to mercury caused F-actin to de-polymerize (Braeckman et al., 1997). Additionally it has been demonstrated that administration of $HgCl_2$ to cells leads to F-actin disruption and fragmentation, causing the formation of blebs which form in response to cell injury (Elliget et al., 1991). In essence, blebs are thought to be the result of the dissociation of the actin cytoskeleton with the plasma membrane, further indicating that F-actin has been damaged when a cell is exposed to mercury (Elliget et al., 1991). Mercury exposure has also been found to trigger an increase in intracellular calcium levels, which in turn functions to activate gelsolin, an actin binding protein that functions to de-polymerize or sever filamentous actin (Yole, et al., 2006). Not surprisingly, rates of F-actin decrease have also been found to correlate to the rate of cell death via apoptosis (Sweet, et al., 2006). Observations regarding the decrease in levels of F-actin were made possible via staining of F-actin with flourescein phalloidin, a toxin that is commonly used in visualizing polymerized actin (Elliget, et al., 1991). G-actin could also be stained in order to visualize the extent of which actin had de-polymerized into its constitutive subunits.The decrease of F-actin can be explained with regards to the actin binding proteins that regulate the stability and integrity of the actin cytoskeleton (Elliget, et al., 1991). It is believed that the function of proteins such as talin, α-actinin, spectrin, and fodrin are inhibited and their binding properties significantly altered when mercury is introduced into their given environments (Elliget, et al., 1991). Spectrin and related proteins are known to playing a role in maintaining actin cytoskeleton structure and association with the cell plasma membrane, while α-actinin is an important protein that helps cross-link actin filaments (Cooper, et al., 2004). Spacing generated by the cross linking properties of α-actinin allows for the binding of myosin to the filaments. The presence of myosin on actin in turn functions to aid in contraction which is important in certain specialized cells such as muscle cells (Cooper, et al., 2004). Interference in the binding of any of these actin-binding proteins can result in the improper function or assembly of the actin cytoskeleton, thereby influencing cellular functions in general.

It is critical that the actin cytoskeleton not be disrupted in nerve cells for if it is, the cells will not carry out their duties properly, and an organism's nervous system as well as its physiological functions, may be severely impaired. In the nervous system, two major classes of cells exist – neurons and glial cells (Kandel et al., 2002). Glial cells play an important role in the proper functioning of the nervous system. They are important in providing support and nutrition, as well as supporting brain structure (Kandel, et. al, 2002). Furthermore, glial cells function to insulate neuronal groups as well as synaptic connections, ensuring that the electric signal is effectively transduced from one neuron to the next and does not dissipate into the extracellular environment (Kandel, et. al., 2002). Additionally, glial cells play major roles in helping clear debris and dead neurons from a particular region and also guide migrating neurons during brain development (Kandel, et. al, 2002). Most interestingly, it has been discovered that neurons are dependent on cholesterol produced in glial cells in order to form multiple and effective synapses (Mauch et al., 2001). Because of these functions and several other vital factors, the study of glial cells is quite important and it is necessary to investigate how F- actin levels and organization within these cells would, upon exposure to mercury, be disrupted and lead to an impairment in the ability of glial cells to carry out their normal functions.

In this experiment, glial cells in an experimental group will be exposed to varying concentrations of mercury chloride ($HgCl_2$) in order to determine what effect mercury has on intracellular F-actin levels in comparison to F-actin levels in control cells, which will not be exposed to any mercury. Cells will be obtained from 11-day old chick embryos via primary tissue culture. These cells will be plated onto cover-slips containing laminin and poly-L-lysine so as to ensure optimal cell growth and viability. Cells will then be fixed onto the cover-slips with fix and fix/perm buffers, and the F-actin of these cells will be stained with Alexa-Fluor 568 phalloidin, a dye that specifically stains filamentous actin a fluorescent red color. Levels of F-actin in glial cells will be determined by quantifying the brightness of pixels after a fluorescent micrograph of cells displaying F-actin will be obtained via fluorescent microscopy. The brightness of the phalloidin label should be proportional to the amount of F-actin since more actin will provide more binding sites to phalloidin, making it brighter in appearance. Because mercury is known to play a role in inhibiting actin assembly, triggering actin cytoskeletal rearrangements and stimulating F-actin de-polymerization, **it is hypothesized that levels of F-actin in glial cells will decrease as concentrations of mercury are increased in the glial cell's environment.**

Materials and Methods

Materials

Glass slides, glass cover-slips, graduated cylinders, tweezers, forceps, scalpels, Nikon-80i Eclipse Microscope with SPOT RT CCD Color Camera (Diagnostic Instruments Inc.), compound light microscope, beakers (varying volumes), SPOT imaging software, ImageJ (1.32j version) imaging software, petri dishes, 10uM mercury chloride – $HgCl_2$ (supplied by Dr. Jani Benoit), 10ml Falcon tubes, 0.5% HCl, HBSS, Pasteur pipettes, micropipettes,

micropipette tips, 1M NaOH, sucrose, 37% formaldehyde, hot plate, stir bars, 25% gluteraldehyde, NaCl, KCl, K_2HPO_4, KH_2PO_4,
L-15, Deoxyribonuclease I – 5mg/ml (Alexa Fluor 488 conjugate from Invitrogen Corp.), Alexa Fluor 568 phalloidin - 300 units/ml (from Invitrogen Corp.), SPF chick eggs: *Gallus gallus* (Charles River Laboratories, Inc.), 25% Triton X-100, kim-wipes, 70% EtOH, 10ml flasks, 35mm Falcon petri dishes, laminin, poly-L-lysine (1mg/ml), valap wax, distilled H20, Macintosh computer (OSX operating system), Canon A20 digital camera, incubating chamber at 37 C, trypsin, 110mm Petri dishes, C-medium, dissection microscope, F+-medium, pH meter (Daigger 5500 pH meter), -20 degrees C refrigerator, tinfoil, stop-watch, nail polish. All tissue culture materials were obtained from Sigma Chemical Co.

Methods

Primary Tissue Culture of Chick Embryonic Sympathetic Neurons
(As described by Primary Culture of Chick Embryonic Peripheral Neurons by
Peter J. Hollenbeck at Purdue University, West Lafayette, IN., and modified by Robert L. Morris at Wheaton College, Norton, MA.)

Chick eggs were obtained from Charles River Laboratories, Inc. and were incubated for 11 days in an incubator pre-set at 37 degrees C. At 11 days of incubation, eggs were removed from the incubator. Soon afterwards, the egg was inverted such that the blunt/flat end of the egg was facing up. This portion of the egg was sprayed with 95% EtOH so as to ensure sterilization. Blunt edged tweezers were obtained and used to cut through the egg shell, approximately 2.5 centimeters from the peak of the blunt edge of the egg. This portion of the shell was removed, thereby exposing the embryo to the air. The embryo was gently lifted up out of the egg with the blunt tweezers and placed in a 110mm petri-dish that contained approximately 3ml of warm HBSS (Hanks Buffered Salt Solution). The head of the embryo was pinched off and placed back in the egg. The body was transferred to a clean 110mm petri dish with 5ml of HBSS. The wings, legs and other limbs and organs of the chick embryo were removed with tweezers and were placed in a localized area of the petri dish. The embryo was then positioned such that its ventral region was positioned in an upwards position, facing the dissector. Tissue surrounding the spinal cord of the embryo was removed with sharp-edged forceps. Dorsal root ganglia were observed soon afterwards, and as much tissue surrounding the spinal cord as possible was removed. The dorsal root ganglia were pulled away from the spinal cord by the root of the cluster, not by the cell body (the round ball). These dorsal root ganglia clusters were placed in a 35mm Falcon petri dish containing 2mL of HBSS. A sympathetic chain was similarly obtained by gently scraping the spinal cord and pulling away at a filamentous chain. This chain was also placed in the 35mm Falcon petri dish.

Preparation of Substrata

Cover-slips were coated with laminin and poly-lysine in the following manner. The inside lid of a sterile 110mm petri dish was obtained. A drop of a 1mg/ml poly-L-lysine solution administered from a glass Pasteur pipette were distributed around the petri dish lid. Sterile cover-slips were obtained, and one cover-slip was placed on each drop of

the poly-L-lysine. The cover-slips were allowed to sit on top of the poly-L-lysine for approximately 1 hour. Afterwards, dH_20 was administered to the petri dish lid in which the cover-slips were sitting, allowing the cover-slips to partially float so that they could be lifted by forceps. The cover-slips were lifted up out of the water and rinsed with sterile dH_20. They were then positioned to sit at a slant on the edge of the petri dish lid, so as to allow the surface onto which poly-L-lysine was administered, to dry. Laminin drops were then administered via a glass Pasteur pipette to the lid of a sterile 110mm petri dish. Once the face of the cover-slip which was exposed to poly-L-lysine had dried, each cover-slip was then positioned down onto a single lamanin drop such that the side of the cover-slip onto which poly-L-lysine had dried, was now touching the lamanin droplet. Cover-slips were allowed to sit on top of these lamanin droplets for one hour. After time was up, HBSS was administered to the lid in which the cover-slips were sitting so as to float them. They were lifted up out of the water with forceps and rinsed with sterile water. They were then placed in a 35mm Falcon petri dish containing 2mL of growth medium so as to keep the cover-slips from drying out before cell plating.

Cell Plating

Ganglia that were moved from the 110mm dissection dish to the 35mm Falcon petri dish containing HBSS, were dissociated in the following manner. Ganglia were washed three times with HBSS by removing HBSS with a Pasteur pipette and adding fresh HBSS with a separate, sterile Pasteur pipette. HBSS was removed after the final wash and replaced with a trypsin solution (Ca/Mg-free HBSS that contained a trypsin concentration of 0.25%). The ganglia were kept in this solution for a period of 15-20 minutes at 37 degrees C. The trypsin solution was then removed and replaced with a HBSS solution with a volume such that there was approximately 1 drop HBSS per ganglion in the petri dish. Ganglia were then triturated gently with a drawn Pasteur pipette so as to dissociate ganglia into individual cells. This cell suspension was mixed with F-medium and distributed amongst dishes containing cover-slips that were ready to support cell growth on the poly-L-lysine and laminin medium. Cells were allowed to grow on the cover-slips for 24 hours at 37 degrees C.

Preparation of Buffers

PBS (Phosphate Buffered Saline) Buffer

To make a 1 liter PBS buffer, a dry, sterile, 1000ml flask was first obtained. A magnetic stir bar was placed at the bottom of the flask. Next, 800ml of distilled, sterile water was added. 80 grams (8% w/v) of NaCl were then added to the flask, followed by 2 grams (0.2% w/v) of KCl, 26.8 grams (2.68% w/v) of K_2HPO_4 and 2.4 grams (0.24% w/v) of KH_2PO_4. This solution was set on a magnetic stir plate and was stirred for approximately 1 hour. 200ml of distilled, sterile water were added to the flask and the solution was stirred an additional 20 minutes. Parafilm was placed over the top of the flask so as to prevent contamination. The solution was then filtered through a 0.22 micron filter and the bottle

in which is was filtered into was capped. Filtered PBS was then brought up to a pH of 7.4 by using a pH meter (Daigger 5500 pH meter) and adding 1 M NaOH until the pH reached the required value.

Fix Buffer

A sterile 250mL flask was obtained and to it, 120mL (94% v/v) of L-15 was added. Next, 6.48mL (5.1% v/v) of 37% formaldehyde was added, followed by 0.48 mL (.37% v/v) of 25% Gluteraldehyde. Finally, 4.8 grams (3.7% w/v) of sucrose was added, as was 1.2mL (.94% v/v) of 0.2 M EGTA. This mixture was brought up to a final pH of 7.0 by adding drops of 1M NaOH. The solution was stirred on a stir plate with a stir bar placed at the bottom of the flask.

Fix/Perm Buffer

A sterile 250mL flask was obtained and to it, 120 mL (92% v/v) of L-15 was added. Then, 6.48mL (5% v/v) of 37% formaldehyde was added, followed by 0.48mL (.37% v/v) of 25% gluteraldehyde, 4.8 grams (3.7 % w/v) of sucrose, 2.4 mL (1.8% v/v) of 25% Triton x 100 (Tx-100), and 1.2 mL (.92% v/v)of 0.2 M EGTA. The pH of this solution was brought up to 7.0 by adding drops of 1M NaOH as needed.

Block Buffer

A 3% block buffer was made by obtaining a sterile 250mL flask and adding to it 100mL of PBS and 3 grams of BSA. This solution was shaken continuously for approximately five minutes to get the BSA as dissolved into solution as possible.

PBS/Triton x 100

This PBS/Triton X-100 solution was prepared by obtaining 500mL of PBS in a sterile 1000mL flask. To this 500mL PBS solution, 10mL of 25% Triton X-100 was added). Solution was mixed via stirring with a stir bar on a stir plate for 10 minutes.

Making up Mercury Chloride Solution

To make up a 100nM $HgCl_2$ solution, the following procedure was followed:

1.) For final solution of 8mL of a 100nM solution, $M_1V_1 = M_2V_2$

M_1 = 10uM
V_1 = ?
M_2 = 100nM
V_2 = 8 mL

V_1 = 80 uL.

80 uL of 10 uM $HgCl_2$ was dissolved in 8mL of HBSS to get 8 mL of 100nM mercury solution.

**See page 02/23/08(56)MJO for calculations of additional concentrations

Preparation of Glia and Neurons

Fixing cells

15 petri dishes containing growing cells were obtained from incubator pre-set at 37 degrees C. The cover of each petri dish was labeled according to the mercury concentrations that would be applied to the cells in each dish. HBSS from each petri dish was carefully withdrawn and replaced with the mercury chloride solution. Cover-slips labeled “0” or “- 0 “ were administered an HBSS solution containing no mercury (3ml to each petri dish) , while cover-slips labeled either “10”, “25”, or “100” received a solution with the corresponding mercury concentration (3mL to each petri dish). Petri dishes were replaced to the 37 C incubator for 20 minutes. After 20 minutes, petri dishes were removed from the incubator. The mercury solution was removed immediately and petri dishes were transferred to a hood. Next, 2mL of the fix/perm buffer was added to each dish via a glass Pasteur pipette and the dishes were incubated at room temperature for 15 minutes. After 15 minutes had elapsed, the fix/perm solution was removed and 2mL of fix buffer were added to each petri dish. The petri dishes were then allowed to incubate at room temperature for another 15 minutes. After this time had elapsed, the fix buffer was removed and 1mL of PBS/Tx-100 solution was added. The PBS/Tx-100 solution was removed from each petri dish, with no incubation step in between. After PBS/Tx-100 solution was removed, 1mL of Block buffer was added. Sodium azide was added to these petri dishes and they were stored over night in a refrigerator.

Actin Fluorescence

Preparation of Fluorescent Stains

It was determined that 0.36 uL of Deoxyribonuclese 1 Alexa Fluor 488 conjugate and 5ul uL of Alexa Fluor 568 Phalloidin was needed for one cover-slip. So, for 15 cover-slips, 5.40 uL of DNase and 75 uL of phalloidin were required. Additionally, 3mL of PBS (200uL/cover-slip) was required to which the phalloidin and DNase would be added. See pages 03/04/08(60)MJO – 03/04/08(61)MJO for calculations of making up these dyes.

Staining Actin

Petri-dishes containing fixed cells were obtained from the refrigerator, where they were stored. A 110mm petri dish lid was obtained. A sizeable portion (5 inches wide by 6 inches long) of parafilm was cut and pressed firmly onto the interior surface of the petri dish lid. This was repeated for two more 110mm petri dish lids. 5 centrifuge caps were placed on each lid and served as pedestals for the cover-slips in humidity chambers. With a glass Pasteur pipette, the block buffer containing sodium azide was removed. The cover-slips were then washed three times with 1mL of PBS

(pH 7.4) by adding 1mL of PBS through a glass Pasteur pipette and simultaneously withdrawing that 1mL PBS with another sterile glass Pasteur pipette. The cover-slips were then carefully lifted up off of the petri dish bottoms with sharp edged tweezers and placed face up (the face on which the fixed cells are on) onto the centrifuge tube caps (pedestals). Next, each cover-slip was flooded with 1mL of the DNase/Phalloidin dye. The cover-slips that were labeled "- 0" and "- 100" were administered PBS instead of the dye. The dye was allowed to sit on the cover-slips for 20 minutes. While this incubation step was occurring, the other half of the petri dish was placed over the lid, so as to prevent moisture from escaping too quickly. After twenty minutes, the cover was removed. Each cover-slip was picked up by a forceps and excess dye was removed by gently tapping each side of the cover-slip onto a dry, sterile kimwipe. The cover-slips were put back into each of their respective 35mm Falcon petri dishes and were rinsed three times with PBS as executed previously. 15 sterile slides were obtained and laid out onto dry paper towels. A drop of PBS was placed onto each slide and each slide was labeled according to which concentration of mercury the cells on the treated cover-slips were exposed to. The cover-slips were inverted such that the side that was just administered with fluorescent dye is facing down, towards the petri dishes. The corresponding concentration number of each cover-slip was placed on top of the PBS droplet of each matching slide with the same concentration number. The four sides of the cover-slip were painted with two coats of nail polish. Finally, the slides were allowed to dry in a dark, cool, location.

Fluorescence Microscopy

A Nikon 80i Eclipse equipped with a SPOT RT Color CCD camera with a 0.76x magnification was used. First, the EXFO X-cite 120 Fluorescence Illumination System was turned on and was set to the highest setting. Next, the SPOT RT Color CCD camera was turned on. This step was followed by turning on the microscope power supply and then the Uniblitz Model VMM-D1 shutter driver. Finally the Mac G4 computer was turned on. After these steps were accomplished, the PHOTO/BINO slider was set to "BINO." Next, the Nomarski analyzer was removed from the light path and the filter turret was set to the "Open" position, followed by setting the fluorescent shutter to "Closed." Thereafter, the objective turret was rotated to the Nikon Plan Fluor 40x/0.75 Ph2 DLL infinity/0.17 WD 0.72 objective. Next, the condenser turret was turned to Ph2 and the condenser aperture was completely opened. It was made sure that any remaining filters in the light path were completely removed. After this was accomplished, the specimen of interest was placed on the stage and was located by scanning the specimen back and forth. Additionally, the microscope was aligned for Koehler illumination. Next, the SPOT imaging program was opened and the phase mode was selected. A phase image was acquired under an automatic exposure condition. The microscope lamp was then covered in order to block all light. Next, the filter turret was rotated to the Nikon B-2E/C Filter cube. A standard AF 488 image (DNase fluorescence) was acquired with a locked exposure time of only 4.5 seconds (Gain 4. 24 Bits per pixel were additional

settings). Additionally, an optimal AF 488 image was acquired whereby exposure time varied in order to obtain an image that best exemplified the filamentous actin (settings were maintained at Gain 4 and 24 bits per pixel). Next, the filter turret was rotated to the Nikon G-2E/C filter cube. A standard AF 568 image (Phalloidin) was acquired. The exposure time for this image was locked at 0.4 seconds (Gain 4. 24 bits per pixel were additional settings). Next, an optimal AF 568 image was acquired whereby exposure time varied and settings were maintained at Gain 4 and 24 bits per pixel respectively. All images taken were saved in the .tiff format.

Quantification of F-actin

Quantification of collected data was done in collaboration with Blair Rossetti, Amanda Rawson and Michael Grimaldi, so as to obtain the most accurate method by which to interpret the data. To quantify the levels of F-actin in control and experimental cells, an optimal AF 568 image was first opened in ImageJ (1.32j version). The background of the image was subtracted by utilizing the “Subtract Background” function under the “Process” menu. A rolling ball radius of 50 was selected, as was the “white background” option. The image was next converted to a black and white mask by selecting the “Threshold” function under the “Binary” function of the “Process” menu. Next, the standard AF 568 of the same image as the optimal was opened in ImageJ. Under “Process”, the “Image Calculator” was selected. “Image 1” was set to the standard image and “Image 2” was the optimal image. The region of interest was roughly selected and then a histogram was obtained by using the “Histogram” function under the “Analyze” menu. The “Copy” button was clicked and Microsoft Excel was opened. “Paste” was then clicked. Next, the mean gray scale values for all pixels except 255 were calculated by the following : Mean GV = Sum(GV*count)/Total sum. This procedure was repeated for every image of interest.

It should be noted that this entire procedure was done three separate times for three trials. However, only one trial (the third one) was used in quantifying and comparing levels of F-actin in control and experimental cells.

Results

The analysis of images depicting control and mercury-treated cells centered around quantifying brightness being given off by the phalloidin dye. Exposure times for both control and experimental sets were maintained at the same levels so as to eliminate exposure time-dependent brightness fluctuation. Control cells were compared only to cells that were exposed to a mercury concentration of 100nM. Cells that were exposed to mercury concentrations of 10nM and 25nM concentrations were not analyzed due to time constraints No statistically significant differences were determined to be present between brightness levels in cells of the control group and cells that were exposed to a 100nM $HgCl_2$ solution. Disregarding standard deviation however, it was found that brightness values were slightly higher (by 0.4 GV) in the experimental group in comparison to the control group.

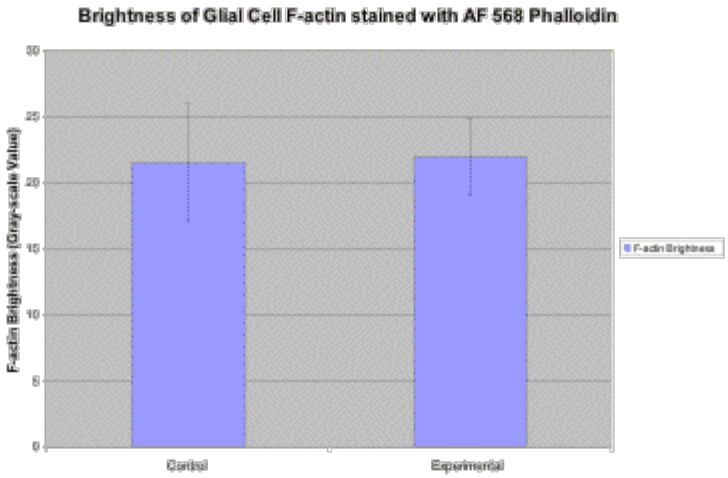

Fig 1. Brightness levels of AF 568 Phalloidin in control cells are the same as brightness levels in cells that were exposed to mercury. The standard deviation values for the brightness values varied between both groups.

Not all images in which glial cells were present were used in the analysis of phalloidin brightness. This is due to the fact that in many of the photographs, neurons were present in association with glia. Analyzing such photographs would give a skewed result, as the brightness of phalloidin in both glia and neurons would be calculated. The averages of brightness values from 15 images in each group, control and experimental, were used in evaluating AF 568 phalloidin brightness. Only those images where the exposure time of fluorescence of the sample was the same for both the optimal image and standard image were used. Where exposure varied between optimal and standard time frames, images of the same cell(s) tended to appear over-exposed when added together and hence, were unreliable for analysis.

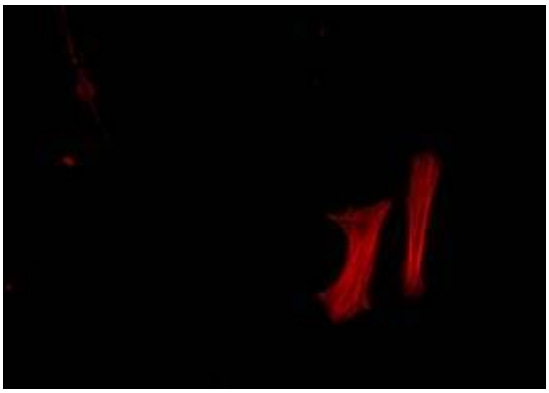

Fig 2. Brightness levels of AF 568 Phalloidin in control glial cells obtained via primary tissue culture of 11-day old chick embryo. Glial cells vastly outnumbered neurons in abundance.

Fig 3. Brightness levels of AF 568 Phalloidin in mercury treated glial cells that were obtained via primary tissue culture of 11- day chick embryo.

No qualitative difference in either cell shape or filopodial abundance was observed between the control and mercury treated glial cells.

Discussion

In this experiment, the hypothesis that F-actin levels in glial cells would decrease as cells are exposed to higher concentrations of mercury, was not supported. Rather we observed no effect of 100nM $HgCl_2$ on F-actin levels in glial cells. Such a conclusion cannot be viewed as authoritative for several reasons. First of all, a very limited number of samples containing glial cells were selected for analysis. Additionally, the method chosen for quantifying brightness of AF 568 Phalloidin was not wholly accurate. This quantification method was dependent on the number of pixels that were below the maximum threshold signal (255), and the background of each image was subtracted so as to minimize background signal as well as cellular background signal. However, it appeared as though this technique was still somewhat area dependent. A gray-scale average (GV) value was found to have changed, albeit very slightly, when the area selected around a glial cell of interest varied. The area that was selected around each cell varied from photo to photo, making analysis of brightness inaccurate. Nevertheless, this was the most precise method that could be implemented. If the standard deviation values for each group were to be smaller, it could be concluded that there is a slight increase in F-actin levels in experimental cells when compared to control cells. Regardless, finding that mercury has no effect on F-actin levels is inconsistent with previous reports.

If for instance, enough credible data was obtained to make the 0.4GV difference between control and experimental trials statistically significant, it could be concluded that mercury is responsible for an increase of F-actin in glial cells. Such an observation could be explained on a molecular and cellular basis by stating that the rate of actin polymerization is faster than the rate at which actin filaments are being damaged as a result of exposure to mercury. Just as ATP-associated actin monomers bind more quickly than nucleotide hydrolysis functions to remove actin

monomers, it can be assumed that as mercury is triggering the de-polymerization of actin, the vast amounts of ATP that are produced as a result of such a process are then binding to now free actin, which is being added to the growing end of an actin filament. In essence, it could be said that the actin filaments and actin cytoskeleton are replenishing themselves at a quicker rate than mercury is functioning to de-polymerize them. Consequently, levels of F-actin in control and experimental cells appeared to be the same. The intermediate concentration of free actin monomers is the same as is the case during treadmilling. So in summary, the mechanism of actin monomer association with the "plus" end of a growing actin filament while exposed to mercury, could be similar to the naturally occurring phenomenon of treadmilling.

A possible explanation as to why $HgCl_2$ had no affect on F-actin levels in experimental cells is due to cell death. Several studies have reported that treatment of various cells with solutions containing mercury may induce programmed cell death, commonly referred to as apoptosis. In fact, one study reports that cell death may be induced by several different pathways upon exposure to various forms of mercury (Yole et al., 2006). It has further been established that exposure to mercury may trigger intracellular levels of calcium to increase, thereby interfering with actin cytoskeleton structure and inducing cell death (Yole et al., 2006). It can be argued that those cells in which F-actin was significantly affected by the mercury, died soon after exposure. The dead cells may not have been sufficiently fixed to the cover-slips and hence, the F-actin could not be stained with the fluorescent dye; therefore, decreased F-actin levels were not observed.

Similarly, it could simply be that $HgCl_2$ did not affect the actin cytoskeleton according to the method by which we administered and exposed the cells. Perhaps the cells were not exposed to the mercury solution for a long enough period of time for any effect to take place. Additionally, it can be argued that different types of cells may have different levels of susceptibility to mercury. Prior studies that looked at the effect of mercury on actin did not use glial cells in their investigations. Thus, glial cells may be less sensitive, and can withstand exposure to mercury more readily than the other types of cells that have been used in the context of this field of research.

Another explanation as to why a 100nM mercury solution did not affect F-actin levels is due to the fact that there may be a certain minimum concentration at which mercury significantly affects F-actin levels intracellularly. One study indeed has found that F-actin de-polymerizes only when cells are exposed to a 500nM mercury solution, and that a concentration lower than this does not seem to produce any significant effect on F-actin structure or abundance (Sweet et al., 2006).

In an attempt to refine this experiment, it would be advisable to use a greater amount cells and a larger data set, such that the difference between the control and experimental groups would be statistically significant. A more accurate

quantification method would be chosen, or the existing one would be improved upon. Furthermore, many more mercury solution concentrations would be tested in order to determine whether or not a decrease in F-actin levels is dose-dependent. This experiment could be further refined by analyzing fluorescently labeled cells immediately after staining, rather than storing slides in the refrigerator. In this manner, the concern over a diminished fluorescence signal would be negated.

Future experiments that could complement the one carried out in this laboratory include analyzing F-actin levels in specific cellular compartments or regions. For instance, it would be interesting to observe how F-actin levels decrease, increase, or remain the same in response to increased mercury levels in structures such as filopodia, which are extremely important in cell signaling, synapse insulation and removal of cellular debris. A comparison between levels of F-actin in filopodia of glial cells and in the axons of neurons could be an enlightening study that would reveal how much actin is required in maintaining these elongated, filamentous structures in a stable and functional state. Another possible future experiment would include looking at how much G-actin is present in the same region of the cell where F-actin has diminished or increased as a result of exposure to mercury. The amount of G-actin would indicate how readily actin filaments are polymerizing or de-polymerizing in response to a cell's exposure to mercury.

References Cited

Alberts, B., Johnson, A., Lewis, J., Raff, M., Roberts, K., Walter, P. Molecular *Biology of the cell. 4th ed.* New York: Garland Science – Taylor and Francis Group, 2002.

Braeckman, B., Simoens, C., Rzeznik, U., Raes, H. 1997. Effect of sublethal doses of cadmium, inorganic mercury and methylmercury on the cell morphology of an insect cell line (Aedes Albopictus, C6/36). *Cell Biology International*. 21(12): 823-832.

Cooper, G.M., Hausman, R.E. *The Cell: a molecular approach*.
Washington, D.C: ASM Press, 2004.

Elliget, K.A., Phelps, P.C., Trump, B.F. 1991.HgCl2 induced alteration of actin filaments in cultured primary rat proximal tubule epithelial cells labeled with fluorescein phalloidin. *Cell Biology and Toxicology*. 7(3): 263 – 280.

Faix, J., Rottner, K. 2006. The making of filopodia. *Current Opinion in Cell Biology*.
18: 18-25.

Grimaldi, Michael, 2008. Personal Communication.

Kandel, E.R., Schwartz, J.H., Jessell, T.M. *Principles of Neural Science – 4th ed*.
New York: McGraw-Hill Companies, 2000.

Kindt, T., Osborne, B., Goldsby, R.A. *Kuby Immunology - 6th ed*.
New York: McGraw-Hill Companies, 2006.

Leong, C.C.W., Naweed, I.S., Lorscheider, F.L. 2000. Retrograde degeneration of neurite membrane structural integrity

of nerve growth cones following in vitro exposure to mercury. *Membrane Biophysics and Biochemistry*. 12(4): 733-737.

Loitto, V.M., Magnusson, K.E. 2004. Hg2+ and small sized polyethylene glycols have inverse effects on membrane permeability, while both impair neutrophil cell motility. *Biochemical and Biophysical Research Communications*. 316: 370-378.

Rawson, Amanda, 2008. Personal Communication.

Rossetti, Blair, 2008. Personal Communication.

Sweet, L.I., Passino-Reader, D.R., Meier, P.G., Omann, G.M. 2006. Effects of polychlorinated biphenyls, hexachlorocyclohexanes, and mercury on human neutrophil apoptosis, actin cytoskeleton, and oxidative state. *Environmental Toxicology and Pharmacology*. 22: 179-188.

Wood, W., Martin, P. Structures in focus – filopodia. 2001. *The International Journal of Biochemistry and Cell Biology*. 34: 726-730.

Yole, M., Wickstrom, M., Blakley, B. 2006. Cell death and cytotoxic effects in YAC-1 lymphoma cells following exposure to various forms of mercury. *Toxicology*. 231: 40-57.